

# Anomalous Photophysics of Bis(hydroxystyryl)benzenes: A Twist on the Para/Meta Dichotomy

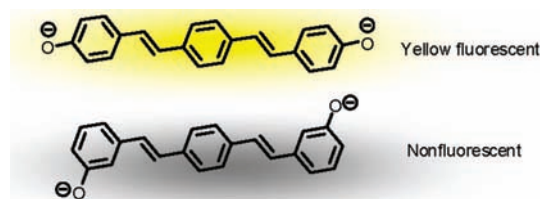
Kyril M. Solntsev, Psaras L. McGrier, Christoph J. Fahrni,\* Laren M. Tolbert,\* and Uwe H. F. Bunz\*

School of Chemistry and Biochemistry, Georgia Institute of Technology, Atlanta, Georgia 30332

uwe.bunz@chemistry.gatech.edu; laren.tolbert@chemistry.gatech.edu

Received March 26, 2008

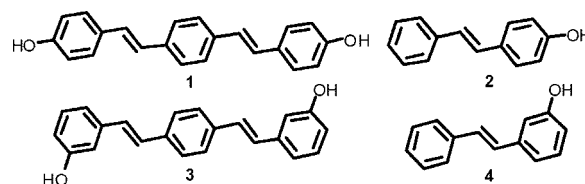
## ABSTRACT



The dianions of two isomeric bis(hydroxystyryl)benzenes show dramatically different photophysical properties.

Stilbenes and distyrylbenzenes represent the first two oligomers leading to poly(*p*-phenylenevinylene) (PPV) and thus are important model compounds for conjugated polymers.<sup>1</sup> As a consequence, there is a significant fundamental interest in the excited-state behavior of these materials. Curiously, *trans*-stilbene (**TS**) is poorly fluorescent, the result of its well-known propensity for isomerization in the excited state.<sup>2</sup> In contrast, *trans,trans*-distyrylbenzene (**TTSB**) and certain derivatives resist isomerization and are strongly fluorescent.<sup>3,4</sup> Recently, Lewis et al.<sup>5</sup> investigated the photoinduced processes in 4-hydroxystilbene (**2**), 3-hydroxystilbene (**4**), and several of their derivatives. The authors observed strikingly different behavior upon excitation, concluding that **4** is a

strong photoacid in water, while **2** does not undergo efficient ESPT (excited-state proton transfer) because of much faster photoisomerization. As a result, both compounds exhibit very weak fluorescence in aqueous solutions.



Given the stronger emissive properties of **TTSB** vs **TS**, we speculated that hydroxyarenes based upon the former might show interesting excited-state proton transfer (ESPT) properties. In this paper, we demonstrate that the excited-state properties of the homologues **1** and **3** are different both from each other and from those of **2** and of **4**, coinciding with the differences between **TS** and **TTSB** in some respects but not in others. Specifically, we show that neither **1** nor **3** is a photoacid. Surprisingly, there is no published literature on the spectroscopy and photoinduced phenomena of either **1** or **3**. In methanol, both **1** and **3** display intensive, single-peak blue fluorescence with a  $\Phi_{fl}$  of 0.37 and 0.62,

(1) Benfaremo, N.; Sandman, D. J.; Tripathy, S.; Kumar, J.; Yang, K.; Rubner, M. F.; Lyons, C. *Macromolecules* **1998**, *31*, 3595–3599.

(2) For leading references, see: (a) Saltiel, J.; Sun, Y. P. *J. Phys. Chem.* **1989**, *93*, 6246–50. (b) Meier, H. *Angew. Chem., Int. Ed.* **1992**, *31*, 1399–1440. (c) Waldeck, D. H. *J. Mol. Liq.* **1993**, *57*, 127–148.

(3) Sandros, K.; Sundahl, M.; Wennerström, O.; Norinder, U. *J. Am. Chem. Soc.* **1990**, *112*, 3082–3086.

(4) Fengqiang, Z.; Motoyoshiya, J.; Nakamura, J.; Nishii, Y.; Aoyama, H. *Photochem. Photobiol.* **2006**, *82*, 1645–1650.

(5) (a) Lewis, F. D.; Crompton, E. M. *J. Am. Chem. Soc.* **2003**, *125*, 4044–4045. (b) Crompton, E. M.; Lewis, F. D. *Photochem. Photobiol. Sci.* **2004**, *3*, 660–668. (c) Lewis, F. D.; Sinks, L. E.; Weigel, W.; Sajimon, M. C.; Crompton, E. M. *J. Phys. Chem. A* **2005**, *109*, 2443–2451.

respectively. Upon preparative photolysis with 355 nm light for 1 h, 3% of the compound **1** interconverted into its *cis,trans*-isomer, while **3** remained unchanged. Similar to hydroxystilbenes, the *bis-para* isomer **1** has somewhat red-shifted spectroscopic features in absorption and emission compared to the *meta* derivative **3** (Table 1). Both **1** and **3**

**Table 1.** Thermodynamic and Photophysical Properties of **1** and **3** in MeOH/H<sub>2</sub>O (2:1 v/v) at 298 K

compd	<b>1</b>	<b>3</b>
$pK_{a1}, pK_{a2}$	$10.1 \pm 0.1, 12.0 \pm 0.1$	$10.6 \pm 0.1, 11.2 \pm 0.3$
species	H <sub>2</sub> A, HA <sup>-</sup> , A <sup>2-</sup>	H <sub>2</sub> A, HA <sup>-</sup> , A <sup>2-</sup>
absorption maxima (nm)	362, 388, 393	355, 359, 363
emission maxima (nm)	428, 575, 533	412, quenched
$\Phi_f$	0.34, n/d, 0.26	0.46 < 0.001
$\tau$ (ns)	0.91, n/d, 1.0	1.41

are soluble in methanol but begin to aggregate in solutions with more than 50 vol % of water. To obtain  $pK_a$  values, all measurements were performed in a 2:1 methanol/water (v/v) mixture,<sup>6</sup> in which both compounds were soluble without apparent aggregation. Figure 1 shows the absorption and

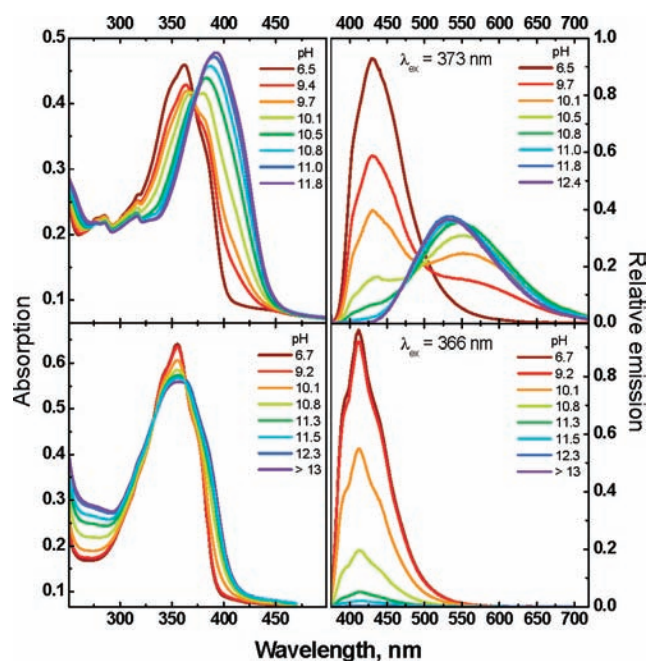


**Figure 1.** Absorption (left column) and emission (right column) spectra of **1** (top row) and **3** (bottom row) in the 2:1 mixture of MeOH/H<sub>2</sub>O (v/v) at different pH values.

emission spectra of **1** and **3**. Upon addition of KOH, the absorption maximum of **1** shifts from 362 nm in the neutral compound to 393 nm in the bis-deprotonated form of **1** (A<sup>2-</sup>) while  $\lambda_{max}$  of **3** shifted from 355 to 363 nm.

To obtain more information about the deprotonation-dependent properties of the two distyrylbenzenes **1** and **3** we analyzed the obtained absorption data (**1** and **3**) using the principal component analysis program SPECFIT.<sup>7</sup> Figure 2 shows the results. The  $pK_{a1}$  values for **1** are  $pK_{a1} = 10.1$

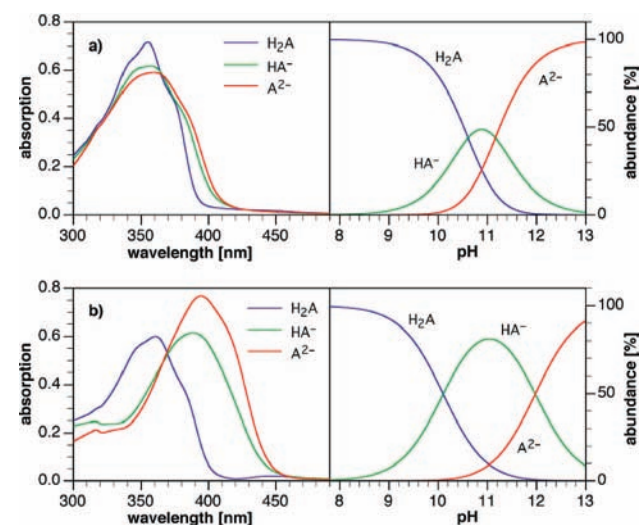


**Figure 2.** Deconvoluted absorption spectra (left) and species distribution diagram (right) for compounds **3** (row a) and **1** (row b).

( $\pm 0.1$ ) and  $pK_{a2} = 12.0$  ( $\pm 0.1$ ), while those for **3** are  $pK_{a1} = 10.6$  ( $\pm 0.1$ ) and  $pK_{a2} = 11.2$  ( $\pm 0.3$ ). The absorption data show nicely that the first deprotonation of **1** is easier than that of **3**, however, the second  $pK_a$  of **1** is almost 0.8 units higher than that of **3**. The difference must be due to the conjugative, mesomeric interactions effective in **1** and its anions, as opposed to the purely electrostatic interactions in **3**, that render its two  $pK_a$ 's more alike.

The  $pK_{a1}^*$  of **1** estimated using a modified Förster method,<sup>8</sup> however, is 1.9, and unlike in more condensed hydroxyarenes, such moderate thermodynamic photoacidity does not lead to detectable ESPT in neutral methanol/water solutions that can compete effectively with the 0.91 ns decay.<sup>9</sup> Therefore, for **1** we do not see any appreciable ESPT, and the  $pK_a$ 's determined from the fluorescence pH-titration simply reflects the ground-state acid–base equilibrium.

From Figure 2, it is clear that upon the first deprotonation of **1** an absorption spectrum results that is close in appearance to that of the dianion A<sup>2-</sup>. However, in emission, the monoanion **1**<sup>-</sup> emission is red-shifted (575 nm) from both the neutral compound (428 nm) and the dianion A<sup>2-</sup> (533 nm). In contrast to the emission, the monoanion of **1** exhibits a blue-shifted absorption from that of A<sup>2-</sup>. We assume that

(6) Canals, I.; Oumada, F. Z.; Roses, M.; Bosch, E. J. *Chromatogr. A* **2001**, *911*, 191–202.

(7) Binstead, R. A.; Zuberbühler, A. D.; Jung, B. *SPECFIT v. 3.0.40*; Spectrum Software Associates: Marlborough, MA, 2007.

(8) Grabowski, Z. R.; Grabowska, A. Z. *Phys. Chem. N.F.* **1976**, *101*, 197–208.

(9) Tolbert, L. M.; Solntsev, K. M. *Acc. Chem. Res.* **2002**, *35*, 19–27.

the anion experiences an intramolecular charge transfer stabilization in the excited-state as the monodeprotonated species is formally a donor–acceptor system, leading to the observed red-shifted emission.

The same experiment, i.e. deprotonation of **3** ( $\lambda_{\text{max}}$  355 nm) to  $\mathbf{3}^{2-}$  leads to a broadening of the absorption and a slight red shift to 363 nm with a red-shifted absorption edge. The emission of neutral **3** is centered at 412 nm. Upon deprotonation its fluorescence is not shifted but quenched. A reliable determination of  $\text{p}K_{\text{a}}^*$  for **3** is problematic due to the complete absence of anion fluorescence.

These observations, i.e., the quenching of the fluorescence of **3** upon deprotonation and the large red-shift of the fluorescence of **1** upon exposure to aqueous base are in stark contrast to the effects visible upon deprotonation of **2** and **4**.<sup>5</sup> On the one hand, **1** shows a much larger red-shift upon deprotonation and its dianion  $\mathbf{1}^{2-}$  is highly fluorescent. On the other hand, dianion  $\mathbf{3}^{2-}$  is weakly fluorescent but its absorption spectrum does not show a significant shift upon exposure to base, similar to the observation for other *m*-hydroxybenzylidene derivatives (*m*-hydroxystilbene<sup>5a</sup> and *m*-hydroxybenzylideneimidazolinone<sup>10</sup>). It is tempting to conclude that the reason for the fluorescence quenching involves twisting about the formal double bond. However, Sandros<sup>3</sup> and Motoyoshiya<sup>4</sup> have observed that distyrylbenzenes undergo adiabatic one-way cis/trans isomerization, producing emission spectra corresponding to the *E/E* forms only. More recently, time-resolved studies indicate the formation of an intermediate but largely planar excited state.<sup>11</sup> Thus, we conclude that twisting leading to quenching does not occur. In the case of stilbene, twisting leads to such decay pathways.

In order to investigate this phenomenon further, we performed quantum chemical calculations (B3LYP/6-311+G(2d,2p)//B3LYP/6-311+G(2d,2p)) upon **1**, **3**, and their respective dianions  $\mathbf{1}^{2-}$  and  $\mathbf{3}^{2-}$ . Figures 3 and 4 and

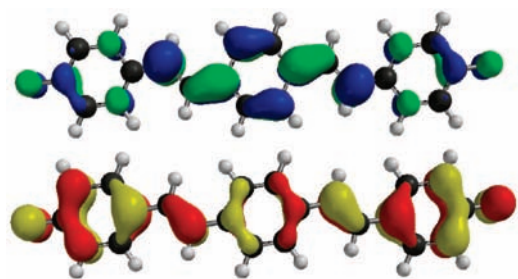


**Figure 3.** LUMO (top) and HOMO (bottom) of  $\mathbf{1}^{2-}$ .

Table 2 show the most salient results. While the neutral compounds **1** and **3** show frontier molecular orbitals (FMO) that are similar to those calculated for distyrylbenzene (see the Supporting Information), the FMOs for  $\mathbf{1}^{2-}$  show larger amplitudes in the two peripheral rings, as a consequence of

(10) Solntsev, K. M.; Poizat, P.; Dong, J.; Rehault, J.; Lou, Y.; Burda, C.; Tolbert, L. M. *J. Phys. Chem. B* **2008**, *112*, 2700–2711.

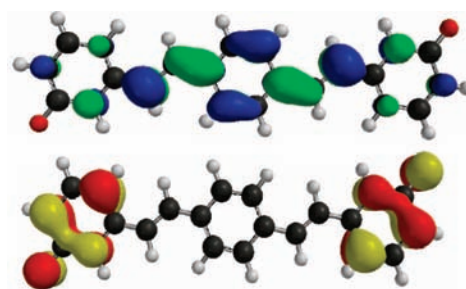


**Figure 4.** LUMO (top) and HOMO (bottom) of  $\mathbf{3}^{2-}$ .

the delocalized phenolate moieties. According to these calculations, the HOMO–LUMO gap decreases upon deprotonation from 3.27 to 2.48 eV.

**Table 2.** Gas-Phase Computational Data for Compounds **1** and  $\mathbf{3}^a$

compd	<b>1</b>		<b>3</b>	
species	H <sub>2</sub> A	A <sup>2-</sup>	H <sub>2</sub> A	A <sup>2-</sup>
S <sub>1</sub> (eV)	3.18	2.48	3.25	1.91
7B <sub>g</sub> →7A <sub>u</sub> <sup>c</sup>	(2.33) <sup>b</sup>	(2.39) <sup>b</sup>	(2.21) <sup>b</sup>	(0.061) <sup>b</sup>
S <sub>6</sub> (eV)				3.13
6B <sub>g</sub> →7A <sub>u</sub> <sup>c</sup>				(1.74) <sup>b</sup>
exp (eV) <sup>d</sup>	3.42 (S <sub>1</sub> )	3.15 (S <sub>1</sub> )	3.49 (S <sub>1</sub> )	3.04 (S <sub>1</sub> ) <sup>e</sup>
				3.42 (S <sub>6</sub> )
HOMO (eV) (7B <sub>g</sub> )	−5.22	0.73	−5.50	0.44
LUMO (eV) (7A <sub>u</sub> )	−1.96	3.21	−2.18	2.69
HOMO–LUMO Gap (eV)	3.27	2.48	3.32	2.26

<sup>a</sup> TDDFT/B3LYP/6-311+G(2d,2p)//B3LYP/6-311+G(2d,2p) level of theory. <sup>b</sup> Oscillator strength in parentheses. <sup>c</sup> Major component of the CI description. <sup>d</sup> Experimental vertical absorption energy. <sup>e</sup> From excitation spectrum.

In the case of **3**, the situation is dramatically different. The HOMO and the HOMO-1 are almost degenerate and localized on the two phenolate rings. In valence bond terms, the two phenolates are disjoint<sup>12</sup> and are electronically only weakly coupled, while the LUMO is extended over the whole  $\pi$ -system but has larger coefficients in the central ring.<sup>13</sup> Given the poor orbital overlap, the HOMO–LUMO transition leading to the lowest singlet excited-state S<sub>1</sub> is expected to exhibit a negligible oscillator strength despite the fact that a B<sub>g</sub> → A<sub>u</sub> transition is symmetry allowed in the C<sub>2h</sub> point group.

A closer inspection of the excited-state manifold obtained from time-dependent density functional theory (TD-DFT) calculations indeed revealed a strong S<sub>1</sub> oscillator strength for neutral **1** and **3** as well as  $\mathbf{1}^{2-}$  but not the *meta*-substituted dianion  $\mathbf{3}^{2-}$  (Table 2). The latter is preferentially excited into

(11) Hsu, F.-C.; Hayashi, M.; Wang, H.-W.; Lin, S. H.; Wang, J.-K. *J. Phys. Chem.* **2007**, *111*, 759–763.

(12) (a) Borden, W. T.; Davidson, E. R. *J. Am. Chem. Soc.* **1977**, *99*, 4587–4594. (b) Properly speaking, “disjoint” refers to diradicals, but the description applies to radical anions and dianions as well.

(13) (a) Wilson, J. N.; Bunz, U. H. F. *J. Am. Chem. Soc.* **2005**, *127*, 4124–4125. (b) Zuccherro, A. J.; Wilson, J. N.; Bunz, U. H. F. *J. Am. Chem. Soc.* **2006**, *128*, 11872–11881.

$S_6$ , while all the lower states exhibit negligible oscillator strengths. Although the quantum chemical calculations offer only estimates for gas phase vertical excitation energies at 0 K, the dominant lowest energy transitions scale linearly with the solution phase experimental data (correlation coefficient 0.994, mean unsigned error 0.01 eV). In agreement with the experiment, the calculations predict a strong bathochromic shift upon deprotonation of **1**, but only a small shift for **3** due to excitation into  $S_6$  rather  $S_1$  (Table 2). The TD-DFT results furthermore indicate a possible nonradiative deactivation pathway through a lower lying triplet  $^3(n-\pi^*)$  state (Figure 5). According to the El-Sayed rule,<sup>14</sup> intersys-

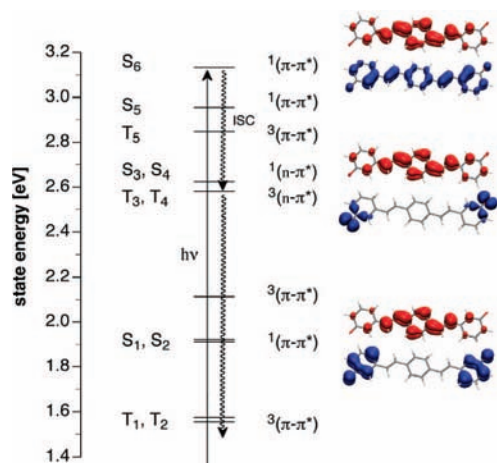


**Figure 5.** Excited-state manifold for dianion  $3^{2-}$  based on TD-DFT calculations (B3LYP/6-311+G(2d,2p)/B3LYP/6-311+G(2d,2p)). Upon excitation into  $S_6$ , nonradiative deactivation may occur through rapid intersystem crossing (ISC) to the  $^3(n-\pi^*)$  states  $T_3$  and  $T_4$ . The surface plots to the right illustrate the  $\pi-\pi^*$  and  $n-\pi^*$  nature of  $S_1$ ,  $S_3$ , and  $S_6$  with the corresponding electron detachment (blue) and attachment (red) densities.

tem crossing from  $^1(\pi-\pi^*)$  to  $^3(n-\pi^*)$  is rapid and typically results in fluorescence quenching due to an increased nonradiative deactivation rate.<sup>15</sup> As illustrated with the electron detachment-attachment densities<sup>16</sup> in Figure 5, the triplet states  $T_3$  and  $T_4$  together with their parent states  $S_3$  and  $S_4$  exhibit  $n-\pi^*$  character involving excitation of a nonbonding oxygen lone-pair electron, thus offering an

efficient nonradiative deactivation channel from  $S_6$  through  $T_3$  and  $T_4$ . Because the calculations indicate that the two  $^3(n-\pi^*)$  states lie above the lowest energy  $^1(\pi-\pi^*)$  state, this nonradiative pathway should not be accessible upon excitation into  $S_1$ . Excitation at the red-edge in the absorption spectrum of  $3^{2-}$  revealed indeed a weak emission band centered around 541 nm, which was not visible with excitation at the absorption maximum (Supporting Information). The corresponding excitation trace acquired at 541 nm peaked at 407 nm and lacked the major higher energy band visible in the absorption spectrum, thus confirming that excitation into  $S_6$  results in nonradiative deactivation without detectable emission from  $S_1$ .

In conclusion, we have demonstrated that the two bis(hydroxystyryl)benzenes **1** and **3** show photophysical properties that are distinct from each other and also distinct from the smaller 3- and 4-hydroxystilbenes **2** and **4**. It is remarkable that the dianion of **1** is highly fluorescent, while the dianion of its isomer **3** is completely nonfluorescent. The large quantum yield of fluorescence of **1**, and its dianion presumably reflects a planarized and quite rigid excited-state with quinoidal resonance contributions,<sup>3</sup> while the quenching of the dianion of **3** may be explained by the presence of an intermediate  $^3(n-\pi^*)$  state combined with a poor Franck-Condon overlap between the HOMO and LUMO of this double phenolate. We recently observed similar phenomena in the case of *p*- vs *m*-dihydroxycruciforms.<sup>17,18</sup> Overall, we find it remarkable that a consanguine group of styryl-based phenols **1–4** display such disparate—and fundamentally interesting—photoinduced effects, not easily predicted by simply examining the structural motifs involved. Such effects, when understood, help illuminate the rather unusual properties of the related cruciforms<sup>18</sup> and may aid in the design of other conjugated fluorophores.<sup>19</sup>

**Acknowledgment.** We thank the Center for Computational Molecular Science and Technology (Gatech), the National Science Foundation (CHE-0456892, L.M.T., K.M.S.; CHE-0750275 U.H.F.B., P.L.M.; CRIF CHE-0443564, C.J.F.), and the National Institutes for Health (DK 68096, C.J.F.) for financial support.

**Supporting Information Available:** Synthetic details for **1** and **3**, a description of the experimental procedures, and titration curves. This material is available free of charge via the Internet at <http://pubs.acs.org>.

OL8006925

(14) (a) Lower, S. K.; El-Sayed, M. A. *Chem. Rev.* **1966**, *66*, 199–241. (b) El-Sayed, M. A. *Acc. Chem. Res.* **1968**, *1*, 8–16.

(15) (a) Brederek, K.; Forster, T.; Oesterlin, H. G. *Luminescence of Organic and Inorganic Materials*; Kallman, H. P., Sprunch, G. M.; Eds.; Wiley: New York, 1962; p. 161. (b) Young, V, Jr.; Quiring, H. L.; Sykes, A. G. *J. Am. Chem. Soc.* **1997**, *119*, 12477–12480. (c) Leray, I.; Lefevre, J. P.; Delouis, J. F.; Delaire, J.; Valeur, B. *Chem.—Eur. J.* **2001**, *7*, 4590–4598. (d) Zhou, Z.; Fahrni, C. J. *J. Am. Chem. Soc.* **2004**, *126*, 8862–8863.

(16) Head-Gordon, M.; Grana, A. M.; Maurice, D.; White, C. A. *J. Phys. Chem.* **1995**, *99*, 14261–14270.

(17) IUPAC names: 4,4'-(1*E*,1'*E*)-2,2'-(2,5-bis((4-*tert*-butylphenyl)ethynyl)-1,4-phenylene)bis(ethene-2,1-diyl)diphenol and 3,3'-(1*E*,1'*E*)-2,2'-(2,5-bis((4-*tert*-butylphenyl)ethynyl)-1,4-phenylene)bis(ethene-2,1-diyl)diphenol.

(18) McGrier, P. L.; Solntsev, K. M.; Schönhaber, J.; Brombosz, S. M.; Tolbert, L. M.; Bunz, U. H. F. *Chem. Commun.* **2007**, 2127–2129.

(19) Hudson, B.; Kohler, B. *Synth. Met.* **1984**, *9*, 241–53.